AN EXPERIMENTAL STUDY OF THE ROLE OF PLASTICITY IN THE RAFTING KINETICS OF A SINGLE CRYSTAL NI-BASE SUPERALLOY

M. Fährmann*, E. Fährmann *, O. Paris**, P. Fratzl**, and T. M. Pollock*
* Department of Materials Science and Engineering, Carnegie Mellon University, Pittsburgh, PA 15213-3890, U.S.A.
** Institut für Festkörperphysik, Universität Wien, Strudlhofgasse 4, Wien A-1090, Austria

Abstract

Directional coarsening in a single crystal Ni-Al-Mo alloy has been studied with varying pre-strain paths that alter the initial state of the $\gamma - \gamma'$ interfaces. These microstructures were generated by pre-straining experiments at intermediate temperatures, maintaining the equiaxed morphology of the precipitates. Their subsequent evolution at high temperatures during ordinary aging as well as stress-annealing was examined by electron microscopy (SEM, TEM) and small-angle X-ray scattering (SAXS). These results are discussed in terms of the connection between the nature of the $\gamma - \gamma'$ interfaces, the local stress state and the resulting driving force for rafting.

Introduction

Rafting, i.e. the directional coarsening of the γ'-precipitates at sufficiently high temperatures under an applied stress, is a well-known phenomenon in single crystal Ni-base superalloys observed under both service and laboratory conditions. Compelling experimental evidence (recently summarized in [1]) shows that the direction and extent of rafting for the given loading condition is controlled by the sign and the magnitude of the $\gamma - \gamma'$ lattice mismatch. This has led to the idea that the superposition of the applied stress with the coherency stresses establishes stress gradients in the microstructure, causing mass flow resulting in rafting. Hence, rafting is expected to occur under conditions where both the γ- and γ'-phases respond elastically to the applied load as modeled in [1-5].

In contrast, in most experiments conducted on alloys of technological significance, rafting has been found to be associated with a finite amount of creep strain [6-14]. Under these conditions, the matrix has been subject to plastic deformation and the $\gamma - \gamma'$ interfaces are no longer fully coherent in the rafted microstructures. Based on these observations, various models accounting for the presence of dislocations have been proposed [7,12,15,16].

Thus, it is still a matter of controversy to what extent the interfacial dislocations affect the driving force and the kinetics of rafting, compared to the behavior when purely elastic conditions prevail. The present work aims to address this problem experimentally by employing various initial microstructures in terms of the state of the $\gamma - \gamma'$ interfaces (fully coherent, partially coherent, isotropically relaxed), and by examining and comparing their subsequent evolution during aging and stress-annealing at high temperatures. This approach permits us to draw important conclusions concerning the microstructural stability of single crystal Ni-base superalloys under creep conditions.

Experimental

Material

The Ni-13.3 at%Al-8.8 at%Mo model alloy employed in this study was provided by PCC Airfoils, Inc. in the form of single crystal slabs approximately 6 mm thick, 100 mm wide, and 150 mm long. The [001] dendritic growth direction was in all instances within 10^{o} of the long axis of the slab. Samples measuring about 25 mm in width were cut from these slabs, and homogenized for 48 hours at 1300 ^{o}C in a protective atmosphere.

On overaged and subsequently quenched samples of the homogenized material the γ'-volume fraction was measured to be 0.60 $\pm$ 0.06 at 980 ^{o}C. The $\gamma - \gamma'$ lattice

Superalloys 1996
Edited by R. D. Kissinger, D. J. Deye, D. L. Anton, A. D. Cetel, M. V. Nathal, T. M. Pollock, and D. A. Woodford
The Minerals, Metals & Materials Society, 1996

mismatch in the same overaged material, where the coherency strains were largely relieved, was measured by X-ray diffraction to be - (0.45 ± 0.05) % in the temperature range of the experiments conducted. Details of the experimental hot stage X-ray diffraction technique will appear elsewhere [17]. Qualitative phase analysis by powder X-ray diffraction did not reveal any detectable amounts of undesirable third phases. However, electron microscopy did show occasional evidence of a needle-like third phase precipitate (presumably δ-NiMo [9]).

The blanks were ground to about 3 mm in thickness, resolutionized in air, quenched, and subsequently aged for 20 minutes at 980 °C. The resulting microstructure consisted of fine scale cuboidal γ'-precipitates of approximately 100 nm mean edge length, embedded coherently in the γ-matrix. Tensile creep specimens with 25 mm gauge length, and compression specimens of approximately 6 mm height, were sectioned from these thin plates by electric discharge machining, and machined to final shape by low-stress grinding.

Pre-straining Experiments

The pre-straining experiments at intermediate temperatures of 850 °C as well as the stress-annealing experiments at the higher temperature of 980 °C were conducted in lever arm creep machines in air. Creep strains in case of the tensile tests were measured by extensometry attached to the shoulders of the specimen. For the compression tests the accumulated creep strain was derived from the reduction in specimen height. The temperature was controlled by two thermocouples in direct contact with the gauge. All samples were cooled under load.

Four different initial microstructures were sought in terms of the state of the γ / γ' interfaces :
(a) fully coherent,
(b) partially coherent, where predominantly the misfit strains in the horizontal (001) matrix channels (with respect to the future [001] loading axis) are largely relieved,
(c) partially coherent with relaxed vertical (100) and (010) matrix channels,
(d) isotropically relaxed, where all {100} type interfaces contain dislocation networks in equilibrated configurations.

State (a) could readily achieved by short-term aging, adjusting the precipitate size to the desired level of ≈ 150 nm suitable for characterization. States (b) and (c) may in principle be accomplished by uniaxial loading in tension or compression along [001]. Based on finite element calculations [12,18], the resolved shear stress for <110>{111} slip in a [001] oriented specimen is expected to be highly dependent on the sense of the load (Fig. 1). An applied tensile stress increases the resolved shear stress for slip in the horizontal matrix channels while reducing the stresses in the vertical matrix channels, for a negative misfit alloy. The situation is reversed under compression. Thus, it was estimated that for an applied stress of 500 MPa along [001], the resolved shear stress would exceed the Orowan stress [7,19] needed to bow slip dislocations into only one set (horizontal or vertical) of the narrow 30 nm matrix channels. The time under load was adjusted such as to approach the secondary creep stage. As will be shown later, under these loading conditions the resolved shear stresses in the ordered γ'-precipitates were still sufficiently low to avoid shearing of the precipitates.

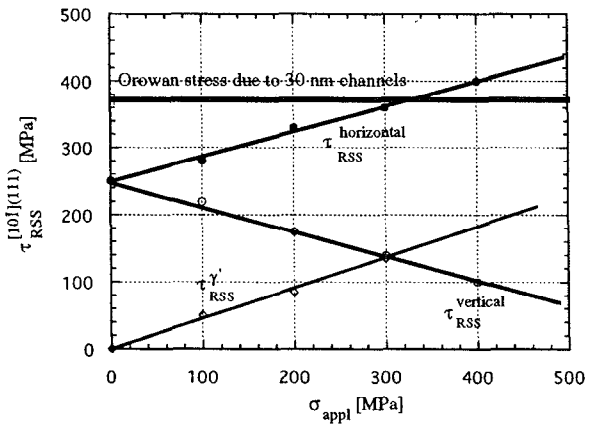

Fig. 1 : Plot of the resolved shear stresses for <110>{111} slip in the horizontal and vertical matrix channels, and the γ'-precipitates, as a function of the applied stress along [001]. Calculations are based on a finite element code [12].

State (d) with its isotropically relaxed interfaces was approximately realized by a two-step thermomechanical treatment : pre-straining in tension, followed by additional pre-straining in compression along the same [001] loading axis. Here the compression specimens were machined from the gauge length of the tensile-tested specimen. Table 1 summarizes the pre-straining conditions employed and the corresponding creep strains accumulated.

Table 1 : Summary of the pre-straining conditions employed to establish different initial microstructures

State	Conditions	Creep Strain
(a)	4 h @ 850 °C	
(b)	4 h @ 850 °C @ 500 MPa^T	≈ 0.03
(c)	4 h @ 850 °C @ 500 MPa^C	≈ 0.05
(d)	4 h @ 850 °C @ 500 MPa^T + 7 h @ 850 °C @ 500 MPa^C	≈ 0.04

T = tension C = compression

Characterization

For all samples tested, sections parallel and transverse to the actual or prior (corresponding to the pre-straining experiment) loading axis were prepared metallographically (electrolytic etching in a solution of 1 wt% ammonium sulfate and 1 wt% citric acid in water), and surveyed in a SEM. Subsequently, TEM specimens were prepared from the same slices by electropolishing employing a solution of 4 % sulfuric acid in methanol at - 24 °C. The TEM foils of (110) orientation permitted location of the [001] loading axis in the corresponding micrograph. The state of the interfaces was assessed by employing various 2-beam diffraction conditions.

In addition to the microscopic examinations, small-angle X-ray scattering was utilized to obtain statistical information about precipitate morphologies in the various micostructures. The SAXS measurements were performed using Cu-K_α radiation and a point collimation system with a sample to detector distance of about 1 m. The intensity scattered in an angular range below 2°, the domain of this technique, was collected with a two-dimensional position sensitive detector with either the (100) or (010) crystallographic plane of the approximately 30 μm thin specimen perpendicular to the incoming X-ray beam. Details of the experimental set-up and the procedure of data evaluation will be published in a forthcoming paper [20]. It is important to note that the SAXS spectra contain information about a much larger number (6 to 7 orders in magnitude) of precipitates than typically sampled by electron microscopy.

Results

Microstructural Evolution during Aging

Fig. 2 displays the characteristic pattern of microstructural evolution during ordinary aging, starting from the various initial microstructures. The inserts are Fourier transforms, calculated by Interactive Data Language software (IDL version IV) from traced and subsequently scanned SEM images, reflecting the crystallographic orientation of the interfaces and the amount of interfacial area perpendicular to a given direction. These Fourier transforms are the 2D analogue to the SAXS spectra from the actually 3D scattering objects, i.e. the precipitates.

The initially fully coherent microstructure (a) coarsens in the capillarity-driven fashion increasing the length scale of the system, with retention of the cuboidal shape of the precipitates. This morphological feature, i.e. the {100} type habit planes, is reflected in the corresponding Fourier transform by two rather sharp streaks into both <100> type directions. Only occasional irregular morphologies are discernible, indicating the beginning of the loss of coherency. Furthermore, the four-fold symmetry of the transform implies that the *average* precipitate shape is square-like in the (100) plane of the image.

The semicoherent initial microstructure (d) displays in the aged condition rather irregular precipitate morphologies. Although the precipitates are not equiaxed, no bias in the direction of coarsening is observed. This is consistent with the symmetry of the corresponding Fourier transform.

In contrast to interfacial conditions (a) and (d), samples with initially partially coherent interfaces exhibit directional coarsening during aging. This is most clearly visible for the sample pre-strained in tension (b) : qualitatively the microstructure evolves *as if* a tensile load was present (for comparison the typical microstructure of samples stress-annealed in tension is shown in Fig. 2e). Due to the emerging predominantly plate-like precipitate morphology oriented perpendicular to the tensile axis, the Fourier transform is now quite asymmetric. It consists mainly of a single streak perpendicular to the broad faces of the plates (the plate-like nature was confirmed by examining all three {100} sections).

In the case of the sample pre-strained in compression (c) the situation is less obvious : precipitates extended along the former [001] compression axis as well as precipitates extended in both <100> directions in the (100) image plane are observed. This complies with the findings of stress-annealing tests in compression [2,12,24], that is, rod-like as well as *two* orientational variants of plate-like precipitates *parallel* to the compression axis, their normals being of <100> type, are found. As a consequence, the asymmetry of the Fourier transforms is less pronounced as compared to the tensile case. Finally we note that in both cases (pre-straining in tension and compression) the resulting aged microstructures appeared to be less perfect compared to their stress-annealed counterparts.

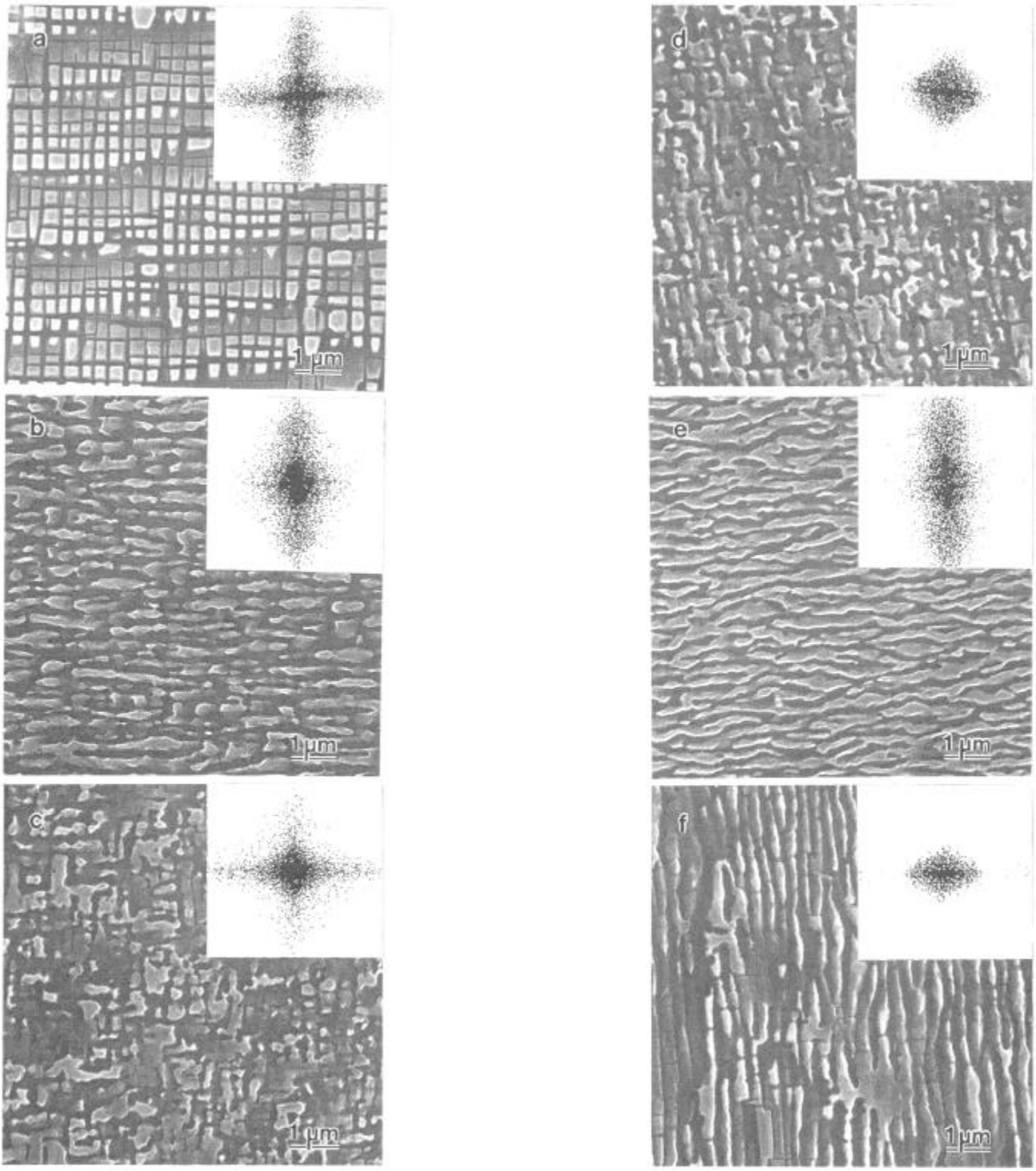

Fig. 2 : SEM micrographs of (100) sections of samples aged 24 hours at 980 ^{o}C, starting with (a) fully coherent $\gamma - \gamma$ interfaces, (b) partially coherent interfaces due to pre-straining in tension, (c) partially coherent interfaces due to pre-straining in compression, (d) semicoherent interfaces. In (e) and (f) typical microstructures of this alloy obtained after stress-annealing in tension and compression, respectively, are shown for comparison. The magnification is the same in all the micrographs.

Microstructural Evolution during Stress-Annealing

In Fig. 3, the evolution of an initially fully coherent microstructure (left column), and of a microstructure pre-strained in tension at 850 °C (middle column), during subsequent stress-annealing at 980 °C under *compression* is shown. The compression axis is vertical in all micrographs. In addition, for comparison purposes, in the third right column the microstructural evolution of the same pre-strained sample during ordinary aging is presented. The corresponding SAXS spectra are arranged in the same order below the micrographs. The components of the scattering vector k_X perpendicular to, and k_Y parallel to the [001] compression axis, are indicated. The scattered intensity is plotted in a logarithmic gray-coded scale.

Starting with a fully coherent microstructure, stress-annealing under compression for one hour under the given loading conditions did not result in any significant morhological changes of the γ'-cuboids. Accordingly, the SAXS spectrum appears four-fold symmetric, and displays streaks into the <100> type directions. After 8 hours under load, however, the cuboids started to transform into plate/rod-like particles parallel to the compression axis. This leads to an asymmetry in the corresponding SAXS spectrum, with the [100] streak now being more pronounced than the [001] streak [25]. For a sample stress-annealed in tension the situation would be reversed [20], with the asymmetry, however, being much more obvious for comparable loading conditions.

The microstructure of the sample pre-strained in tension evolves during the first hour under compression apparently such that still a slight directional coarsening *perpendicular* to the [001] compression axis occurs, as also suggested by the SAXS spectrum. Later on, the microstructure appears disintegrated, showing no signs of directional coarsening. Consistent with this microscopic observation, the corresponding SAXS spectrum is then nearly isotropic. The microstructure of the same pre-strained sample during ordinary aging follows the pattern described in the previous section, i.e. evolving into plate-like particles perpendicular to the *former* tensile axis. This is corroborated by the SAXS spectrum showing a pronounced streak into the [001] direction.

Interestingly, all SAXS spectra obtained with the pre-strained samples are much broader in terms of streak widths as compared to the spectra obtained with the initially fully coherent samples. This indicates [20] that the $\gamma - \gamma'$ interfaces in the pre-strained and subsequently annealed / stress-annealed samples are crystallographically less planar. TEM observations showed that the interfaces in the formerly coherent microstructure were still predominantly of {100} type even after 8 hours under compression (Fig. 4a), whereas starting with a pre-strained sample led to rounded irregular interfaces decorated with interfacial dislocations (Fig. 4b).

Despite the less defined nature of the $\gamma - \gamma'$ interfaces in the pre-strain series, it was still possible to extract useful information from the SAXS spectra in case of the 1 hour samples. The data evaluation is based on the concept of the total interfacial areas $S^{\{100\}}$ parallel or nearly parallel to the {100} planes. The ratio $S^{(001)} / S^{(100)} \approx S^{(001)} / S^{(010)}$ can then be identified with an *average* aspect ratio of the precipitates referred to as ρ_{SAXS} [20]. In addition, we performed semi-automatic image analyses (also described in greater detail in [20]) of TEM DF images, taken from the same microstructures, to obtain a similar parameter ρ_{TEM}. Thus, for plates evolving normal to the [001] applied stress, above definitions of ρ result in values larger than 1.

In terms of the evolution of precipitate aspect ratios (Table 2), the two most notable findings are : (1) the *initially* greatly *enhanced* rate of rafting in the pre-strained sample even under no applied stress, compared to the sample exhibiting initially coherent interfaces, (2) the, albeit small, but resolvable *initial increase* in ρ for the pre-tensioned sample subject to subsequent compression. This trend is *opposite* to what is usually expected in a stress-annealing test in compression with this alloy. We note that the pre-strained sample was heated in the creep frame under full compressive load before conducting the 1 hour isothermal stress-annealing treatment, thus prohibiting rafting due to thermal exposure as described in the previous section.

Table 2 : Summary of the quantitative evaluation of the SAXS spectra and TEM micrographs regarding the average precipitate aspect ratio after 1 hour stress-annealing. The first value refers to SAXS, the second (in parenthesis) to TEM.

	Fully coherent Compression / Tension	Pre-strained in tension Compression / Aged
ρ_{start}	1.2 ± 0.2 (1.3 ± 0.1)	1.6 ± 0.2 (1.4 ± 0.1)
ρ_{end}	1.2 ± 0.2 / < 1.8	2.1 ± 0.2 / 2.7 ± 0.2 (1.8 ± 0.2) / (2.3 ± 0.2)

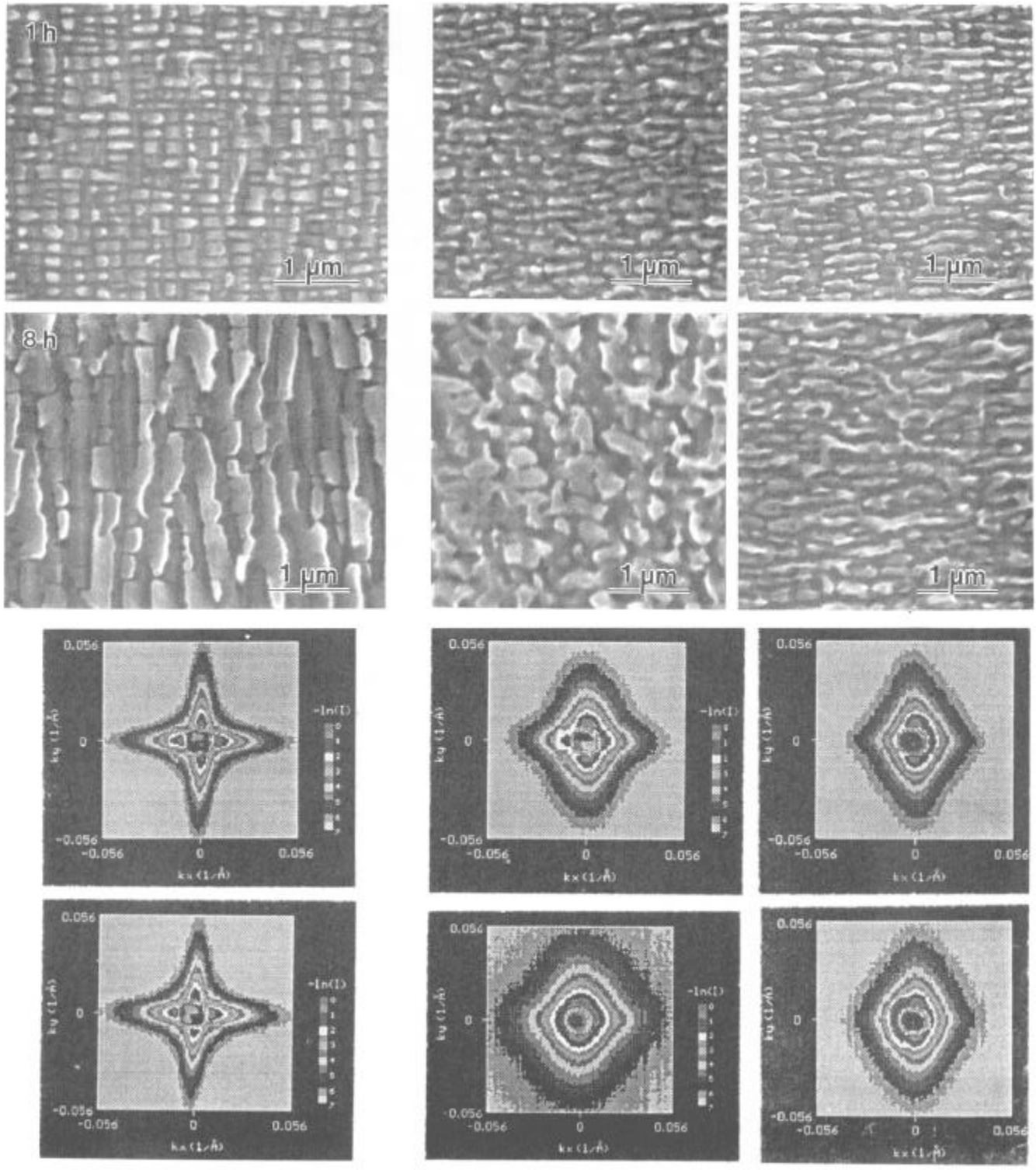

Fig 3 : SEM micrographs ((110) sections) and corresponding SAXS spectra of samples stress-annealed in compression. Left column : initially fully coherent interfaces. Middle column : initially partially coherent interfaces due to pre-straining in tension. The right column shows the microstructure and SAXS spectra obtained after ordinary aging of the same pre-strained sample. The magnification is the same in all the micrographs. The loading direction, if applicable, is perpendicular.

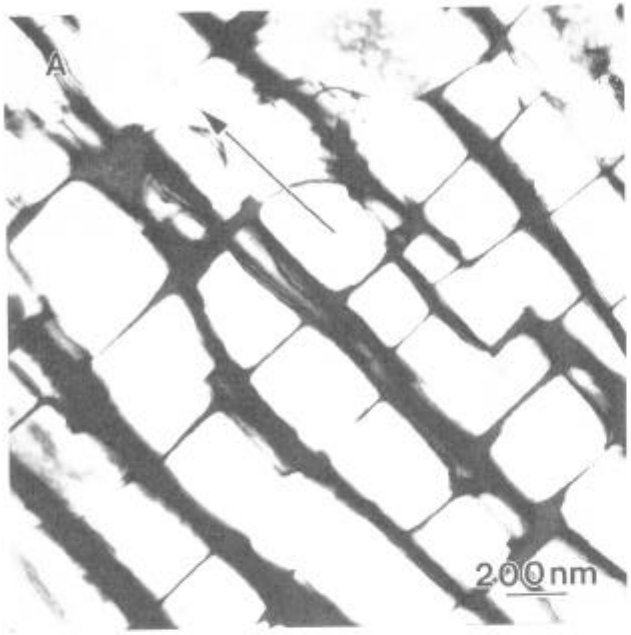

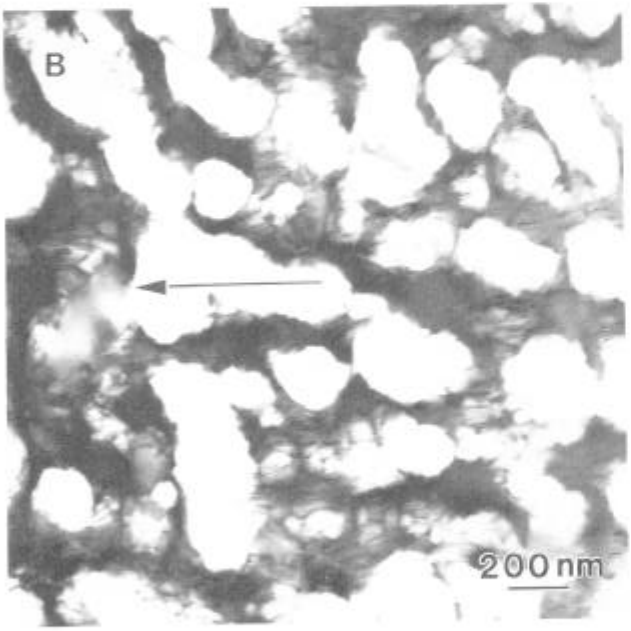

Fig. 4 : Dark-field (DF) images (g=110) of samples stress-annealed for 8 hours at an applied compressive stress of 130 MPa, starting with (a) fully coherent interfaces, (b) partially coherent interfaces due to pre-straining in tension. The direction of the compression axis is indicated by arrows in the micrographs.

Discussion

The experimental results presented provide strong evidence that the kinetics *and* the driving force of rafting are both greatly affected by the state of the $\gamma - \gamma'$ interfaces which in turn is related to the creep deformation. This conclusion is primarily based the observations that

(a) the microstructure in the pre-strained samples rafted even under *no* applied stress in a direction corresponding to the *former* loading axis.

This observation corroborates recent findings by Veron et al. [21] with another single crystal superalloy, and extends their pre-strain compression experiments to all four conceivable initial situations in terms of the state of the $\gamma - \gamma'$ interfaces.

(b) the microstructure in a sample pre-strained in tension rafted under an applied compressive stress *initially* in a direction *opposite* to what is generally observed in compression in this alloy.

Thus, any discussion of the effect of matrix plasticity in rafting in single crystal superalloys *only* in terms of an enhanced kinetics due to the supply of fast diffusion paths is *incomplete*, and misses the important fact that matrix plasticity can profoundly alter the magnitude and direction of the driving force for rafting. Moreover, it is not the presence of dislocations per se, but their arrangement in the various matrix channels which determines the magnitude of the effect. This was realized first by Carry and Strudel [7], and has been subsequently refined in [12,15,16]. The main idea is that slip dislocations deposited on the $\gamma - \gamma'$ interfaces during creep and their subsequent reaction and rearrangement by climb leads, at least partially, to a reduction of the misfit strains in certain sets of matrix channels, while aggravating them in other sets.

In this context the experimental findings regarding the microstructural evolution of the various pre-strained samples during stress-free aging (Fig. 2) can be rationalized : the total strain energy of the single crystal is substantially reduced by eliminating the highly stressed matrix channels. This is accomplished by directional flow of "γ' - material" into those matrix channels, leading to the observed rafting as shown schematically in Fig. 5. In the case of the fully coherent (Fig. 2a) and ideally fully relaxed interfaces (Fig. 2d) no such strain energy gradient exist. Hence, no directional coarsening is observed during stress-free aging.

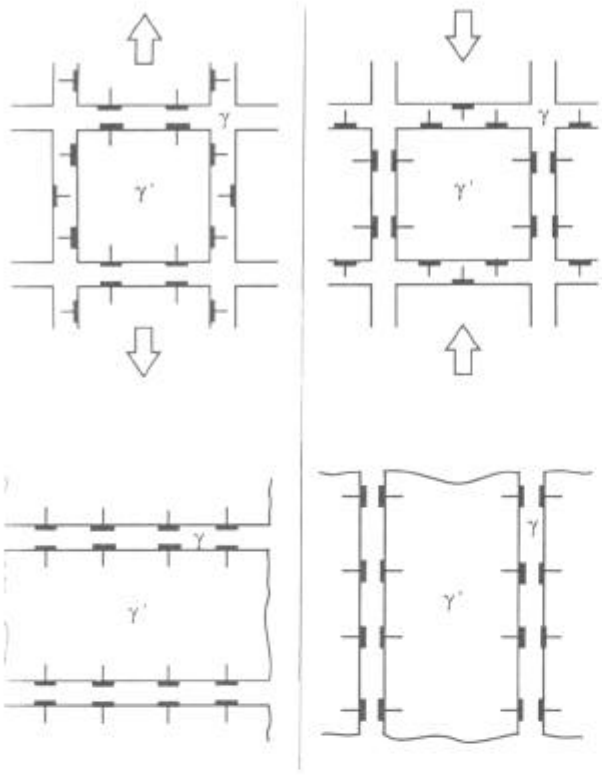

Fig. 5 : Schematic sketch of the dislocation arrangement in the pre-strained samples, and the subsequent microstructural evolution during aging.

This picture (a similar version has been proposed by Veron et al. [21] assuming, however, one set of channels to be dislocation-free) is quite simplistic. We note that the schematic of the initial partially coherent microstructures (Fig. 5) assumes that the misfit strains in certain matrix channels are and remain ideally relieved by virtue of misfit dislocation networks residing at the interfaces. Under the choosen conditions (see Table 1), a high density of interfacial dislocations on e.g. the horizontal (001) interfaces of the pre-tensioned sample is observed as expected (Fig. 6a). However, the reaction and rearrangement of the slip dislocations by climb processes has rarely led to the characteristic misfit strain relieving networks as described in [22,23]. After sufficient thermal activation, e.g. aging for 20 hours at 980 °C (Fig. 6b), significant rearrangement by climb has occurred. Then, however, the precipitates were no longer of cuboidal shape. Apparently only a fairly narrow experimental window in time and strain exists for a given alloy to study such pre-strain effects.

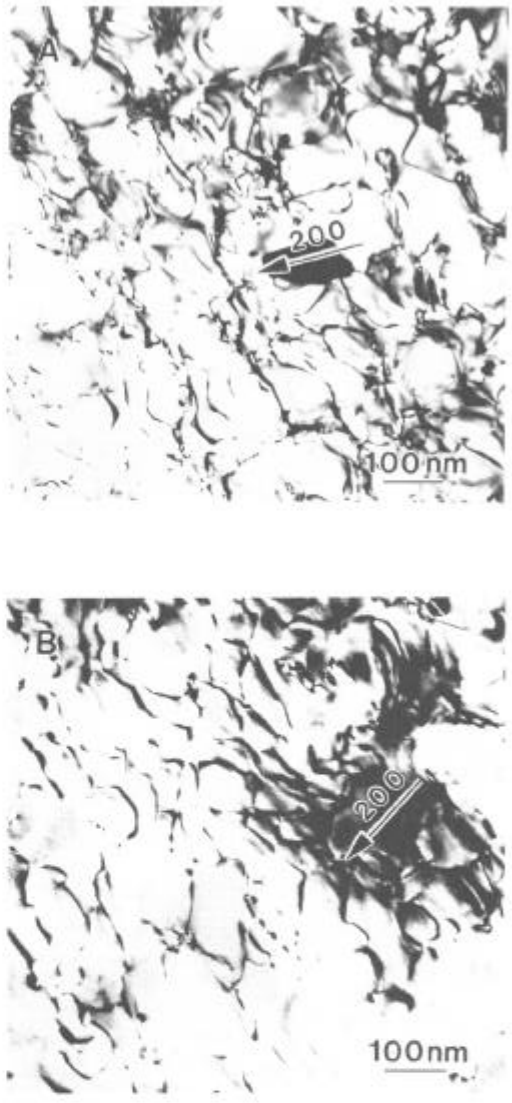

Fig. 6 : TEM bright-field images (g=200) of the dislocation arrangement on (001) interfaces in the sample pre-strained in tension (a), and the same sample annealed additionally for 20 hours at 980 °C.

The interpretation of the second crucial experimental result, i.e. the initially "wrong" direction of rafting in the sample pre-strained in tension under subsequent compression, follows the same line of thinking. Due to the pre-straining in tension, many dislocations deposited onto the (001) interfaces and their reaction products will to some extent relieve the misfit strain locally. Thus, they are arranged in an energetically favorable fashion, and are not expected to leave the interface upon reversal of the applied stress. The interfacial dislocations on the (100) and

the applied stress, misfit strain diminishing arrangements of interfacial dislocations will then gradually build up also at the vertical interfaces.

If this is true, a certain initial time span under compressive applied stress can be expected during which the relaxation of the misfit strains in the various channels is still dominated by the former tensile pre-strain experiment. This is the time span where principally rafting in the "wrong" direction could take place. During prolonged stress-annealing in compression this initial gradient will be substantially reduced, if not reversed. Apparently, after 8 hours of stress-annealing (Fig. 4b), an intermediate stage has been reached in this alloy, the interfaces being uniformly wrapped by dislocations.

In spite of the simplifying assumptions which were made, we believe that this model reflects essential elements of rafting in single crystal Ni-base superalloys. A thorough thermodynamic treatment would have to couple the chemical potential of the various alloying elements with the local stress state in the material, and to account for multicomponent diffusion in the mass flow problem. This was beyond the scope of the present work. Nevertheless, several technologically relevant conclusions can been drawn regarding the microstructural stability of single crystal superalloys under creep conditions :
(a) it is not the high magnitude of the coherency stresses built into the microstructure, but their anisotropic relaxation during creep deformation which ultimately generates the gradients driving rafting;
(b) alloying additions which slow down Ostwald ripening in the alloy, would at the same time be potent candidates to retard rafting since in both cases crossing fluxes of "γ - formers" (such as Cr, Mo, Re ...) and "γ' - formers (such as Al, Ti, Ta ...) are required to accomplish the redistribution of the phases in the microstructure.

Summary

Directional coarsening in a single crystal Ni- 13.3at%Al-8.8at%Mo alloy has been studied with varying pre-strain paths that alter the initial state of the $\gamma - \gamma'$ interfaces. These microstructures were generated by pre-straining experiments in uniaxial tension / compression along [001] at intermediate temperatures of 850 °C, maintaining the equiaxed morphology of the precipitates. Electron microscopy and small-angle X-ray scattering were employed to examine the microstructural evolution during subsequent ordinary aging and stress-annealing at the higher temperature of 980 °C.
The two most important observations are :
(a) the microstructure in samples pre-strained in tension or compression rafted during subsequent aging in a direction as if the former load was still present, whereas a sample with isotropically relaxed interfaces did not show directional coarsening;
(b) the microstructure in a sample pre-strained in tension rafted under an applied compressive stress initially in a direction opposite to what is generally observed in compression for this alloy.

These experimental results provide strong evidence that the driving force for rafting can be greatly affected by matrix plasticity. The anisotropic relaxation of misfit strains in the initially highly stressed matrix channels due to deposition of slip dislocations onto the interfaces and their subsequent rearrangement, appears to be the key for an understanding of rafting during creep of single crystal superalloys.

Acknowledgments

Financial support by the "Österreichischer Fonds zur Förderung wissenschaftlicher Forschung" FWF S5601, the Deutsche Forschungsgemeinschaft, Grant FA 290/1-1, General Electric Company, and the National Science Foundation through Grant DMR 9258297, is gratefully acknowledged. We wish to thank J. Wolf and A. Boegli for conducting X-ray diffraction work and measuring the γ'-volume fraction, and S. Mahajan for helpful discussions.

References

[1] J. C. Chang and S. M. Allen, *J. Mater. Res.* **6**, 1843 (1991).
[2] J. K. Tien and S. M. Copley, *Metall. Trans.* **2**, 219 (1971).
[3] A. Pineau, *Acta metall.* **24**, 599 (1976).
[4] W. C. Johnson, *Metall. Trans.* **A 18**, 233 (1987).
[5] T. Miyazaki, K. Nakamura, and H. Mori, *J. Mater. Sci.* **14**, 1827 (1979).
[6] C. Carry and J. L. Strudel, *Acta metall.* **25**, 767 (1977).
[7] C. Carry and J. L. Strudel, *Acta metall.* **26**, 859 (1978).
[8] D. D. Pearson, B. H. Kear, and F. D. Lemkey, in : *Creep and Fracture in Engineering Materials Structures*, eds. B. Wilshire and D. R. J. Owens, Pineridge Press Ltd., Swansea, UK, 1981, p. 213.
[9] R. A. MacKay and L. J. Ebert, *Scripta metall.* **17**, 1217 (1983).
[10] M. V. Nathal, *Metall. Trans.* **A 18**, 1961 (1987).

[11] U. Glatzel and M. Feller-Kniepmeier, *Scripta metall.* **23**, 1839 (1989).
[12] T. M. Pollock and A. S. Argon, *Acta metall. mater.* **42**, 1859 (1994).
[13] H.-A. Kuhn, H. Biermann, T. Ungar, and H. Mughrabi, *Acta metall. mater.* **39**, 2783 (1991).
[14] Z. Peng, U. Glatzel, T. Link, and M. Feller-Kniepmeier, *Scripta Materiala* **34**, 221 (1996).
[15] S. Socrate and D. M. Parks, *Acta metall. mater.* **41**, 2185 (1993).
[16] J. Y. Buffiere and M. Ignat, *Acta metall. mater.* **43**, 1791 (1995).
[17] M. Fährmann, J. Wolf, and T. M. Pollock, *Mat. Sci. Eng.* A **210**, 8 (1996).
[18] L. Müller, U. Glatzel, and M. Feller-Kniepmeier, *Acta metall. mater.* **41**, 3401 (1993).
[19] T. M. Pollock and A. S. Argon, *Acta metall. mater.* **40**, 1 (1992).
[20] O. Paris, M. Fährmann , E. Fährmann , T. M. Pollock, and P. Fratzl, submitted to Acta Materiala, (1996).
[21] M. Veron, Y. Brechet, and F. Louchet, *Scripta Materiala* , (1996), in press.
[22] R. D. Field, T. M. Pollock, and W. H. Murphy, in : *Superalloys 1992*, eds. S. D. Antolovich et al., TMS Society, Warrendale, PA (1992), p. 557.
[23] R. R. Keller, H. J. Maier, and H. Mughrabi, *Scripta metall. mater.* **28**, 23 (1993).
[24] M. V. Nathal and L. J. Ebert, *Scripta metall.* **17**, 1151 (1983).
[25] M. Fährmann , *unpublished results.*